SCIENTIFIC REPORTS
nature research

OPEN

A machine learning framework for multi-hazards modeling and mapping in a mountainous area

Saleh Yousefi[1], Hamid Reza Pourghasemi[2]✉, Sayed Naeim Emami[1], Soheila Pouyan[2], Saeedeh Eskandari[3] & John P. Tiefenbacher[4]

This study sought to produce an accurate multi-hazard risk map for a mountainous region of Iran. The study area is in southwestern Iran. The region has experienced numerous extreme natural events in recent decades. This study models the probabilities of snow avalanches, landslides, wildfires, land subsidence, and floods using machine learning models that include support vector machine (SVM), boosted regression tree (BRT), and generalized linear model (GLM). Climatic, topographic, geological, social, and morphological factors were the main input variables used. The data were obtained from several sources. The accuracies of GLM, SVM, and functional discriminant analysis (FDA) models indicate that SVM is the most accurate for predicting landslides, land subsidence, and flood hazards in the study area. GLM is the best algorithm for wildfire mapping, and FDA is the most accurate model for predicting snow avalanche risk. The values of AUC (area under curve) for all five hazards using the best models are greater than 0.8, demonstrating that the model's predictive abilities are acceptable. A machine learning approach can prove to be very useful tool for hazard management and disaster mitigation, particularly for multi-hazard modeling. The predictive maps produce valuable baselines for risk management in the study area, providing evidence to manage future human interaction with hazards.

Human interactions with natural extreme events, or hazards, are increasing globally[1]. Natural disasters have affected people and natural environments generating vast economic losses around the world. However, in some developed counties disasters have been decreasing since 1900[2,3].

Hazard is the probability of occurrence in a specified period and within a given area of a potentially damaging of a given magnitude[4,5]. The definition incorporates the concepts of location (where?), time (when, or how frequently?) and magnitude (how large?). Total risk (R) means the expected number of lives lost, person injured, damage to property, or disruption of economic activity due to a particular natural phenomenon, and is therefore the product of specific risk (RS) and elements at risk (E)[6]. In addition, RS is the expected degree of loss due to a natural phenomenon.

Landscapes around the world are reflections of diverse natural processes. The probabilities of extreme natural events are typically greater in more natural areas and are, in fact, extensions of natural systems. Exposure of people to these extreme natural processes could be reduced and limited if predictive models based on new approaches and deeper knowledge of effective factors were employed[7]. Mountainous areas are commonly sites of snow avalanches[8,9], landslides[4,10], floods[11,12], mudflows[13], ice avalanches[14], soil erosion[15–17], rock falls[18], and wildfires[19–24].

Most studies focus on a single hazard, even when there are multiple hazardous processes affecting the same landscapes[8,25–30]. However, hazards sometimes interact with each other. Sometimes, the mitigation of one

[1]Soil Conservation and Watershed Management Research Department, Chaharmahal and Bakhtiari Agricultural and Natural Resources Research and Education Center (AREEO), Shahrekord, Iran. [2]Department of Natural Resources and Environmental Engineering, College of Agriculture, Shiraz University, Shiraz, Iran. [3]Forest Research Division, Agricultural Research Education and Extension Organization (AREEO), Research Institute of Forests and Rangelands, Tehran, Iran. [4]Department of Geography, Texas State University, San Marcos, TX 78666, USA. ✉email: hr.pourghasemi@shirazu.ac.ir

hazardous process may intensify another's frequency, duration, distribution, or intensity[31]. Studying natural hazards separately, especially in mountainous regions, may produce miscalculations of risk (or the probability of occurrence of the specific extreme natural event) in those areas. Multi-hazard risk assessment (the collective likelihood of experiencing an extreme natural event among a set of hazards) could be useful for controlling the interactions of hazards[32].

Snow avalanches, landslides, wildfires, land subsidence, and floods are the most important risks in many mountainous regions of the world[8,18,33,34]. These five hazards can impact and interrupt systems (transportation, electrical power, water provisioning systems, and others), processes (trade, travel, extraction, shipping), places (residential areas, commercial districts, industrial areas, recreational sites), and people in risk-prone areas[33,34]. Multi-hazard risk mapping is an important need for land use management at provincial and national scales[4,33–37]. Multi-hazard mapping is receiving increasing attention[1,7,38–45]. Multi-hazard analysis has been conducted in mountainous regions of Iceland, New Zealand, Iran, and Tajikistan. In Iceland, a general method was developed for analysis of snow avalanche, rock-fall, and debris-flow hazards[7]. Schmidt et al.[46] developed an approach for multi-risk modeling in New Zealand, creating an adaptable software prototype that allows researchers to 'plug in" natural processes of interest. Pourghasemi et al.[45] undertook a multi-hazard risk assessment based on machine learning methods in Fars Province, Iran. They considered floods, forest fires, and landslides in their study area. In another study, multiple hazards (rockslides, ice avalanches, periglacial debris flows, and lake-outburst floods) were assessed in a mountainous region of Tajikistan to develop a comprehensive regional-scale map of hazards for the study area[47].

Though these studies exemplify multi-hazard mapping, a comprehensive study on multi-hazard assessment by machine learning models is lacking for mountainous areas. The development of multi-hazard risk mapping approaches using new methods is critical for effective management of hazards in some regions. Iran, in fact, is a country that has an extensive array of hazards (flood, landslide, earthquake, drought, dust storm, soil erosion, snow avalanche, etc.) due to the diverse geomorphological and climatic zones[28,12,48–50]. Snow avalanches, landslides, subsidence, wildfires, and floods occur annually in the Zagros and Alborz mountain chains in Iran; people are more numerous in these regions than in other parts of the country[51–54]. In this study, five major natural events (flood, landslides, land subsidence, snow avalanches, and wildfires) in Chaharmahal and Bakhtiari Province provide the basis for a multi-hazard risk assessment map. The main objective is to evaluate machine learning models as useful, universal, and accurate multi-hazard mapping products that can be applied by land use managers and planners. Based on a review of the literature, we have selected a set of machine learning models including; generalized linear model (GLM)[55–57], random forest (RF)[17,58,59], a support vector machine (SVM)[60–62], boosted regression trees (BRT)[63–65], mixture discriminate analysis (MDA)[66,56], multivariate adaptive regression splines (MARS)[67,56,68], and functional discriminant analysis (FDA)[17,66] for multi-hazard mapping. Finally, based on the accuracies of the models, available data, and the sources of models, the SVM, GLM and FDA algorithms were used to map hazards in the study area.

Study area. Chaharmahal and Bakhtiari Province is in southwestern Iran (Fig. 1). It is defined by a rectangle with sides at 31° 9′ and 32° 38′ N and 49°30′ and 51° 26′ E. The province contains ten counties (Ardal, Borojen, Shahrekurd, Farsan, Lordegan, Kiar, Khanmirza, Kohhrang, Ben and Saman) and covers an area of 16,553 km^2 (1% of Iran). Elevation ranges from 778 m to 4,203 m above sea level and the mean elevation in the province is 2,153 m, making it the highest province in Iran. The population of the province is 947,000. Floods, mass movements, land subsidence, wildfires, and snow avalanches occur here regularly[69].

Methodology. This study involved three main activities (Fig. 2): (1) Collection of extreme event data through extensive field work and assessments of government reports over a 42-year period (1977–2019); (2) Identification of the most important effective factors for each hazard through a literature review; (3) Hazard modeling using a generalized linear model (GLM), a support vector machine (SVM) model, and a functional discriminant analysis (FDA) model and construction of multi-hazard risk maps (MHRM) using the models that were most accurate for each hazard.

Hazards data inventory. This study identified 3,455-point locations signifying the sites of five types of extreme hazardous events that occurred over a 42-year period in the Chaharmahal and Bakhtiari province through field surveys and examination of scientific reports (Fig. 3). These events included 246 snow avalanches, 97 wildfires, 346 floods, 868 landslides, and 1902 cases of land subsidence. The machine learning models in this study required data from both hazard and non-hazard locations to conduct modeling. Equal numbers of non-hazard locations were randomly sampled to balance the hazard locations[21–23,66,70]. The samples were divided into two groups for training (70%) and for validation (30%)[21,23,24].

Data collection of the effective factors for five hazards. Based on both a review of previous studies and a compilation of experts' suggestions, effective factors for each hazard were measured and mapped in raster layers of 10 × 10 m pixel size in ArcGIS 10.4.2. The effective factors (Table 1) fell into five categories: topography (DEM, slope, topographic wetness index, plan curvature, aspect, and convergence index), geology (lithology and distance from a fault), hydrology and climatology (precipitation, distance from a river, groundwater depth, drainage density, absolute minimum temperature, wind exposure index, absolute maximum temperature, and snow depth), society (distance from a road and distance from an urban areas), and vegetation/land cover (land use and NDVI). The topographic factors were extracted from 1:25,000 topographic maps obtained from the Iranian National Cartographic Center. The geological factors were acquired from a geologic map at a scale of 1:100,000, acquired from the Iranian Geology Organization. Hydrological and climatic factors were measured using data

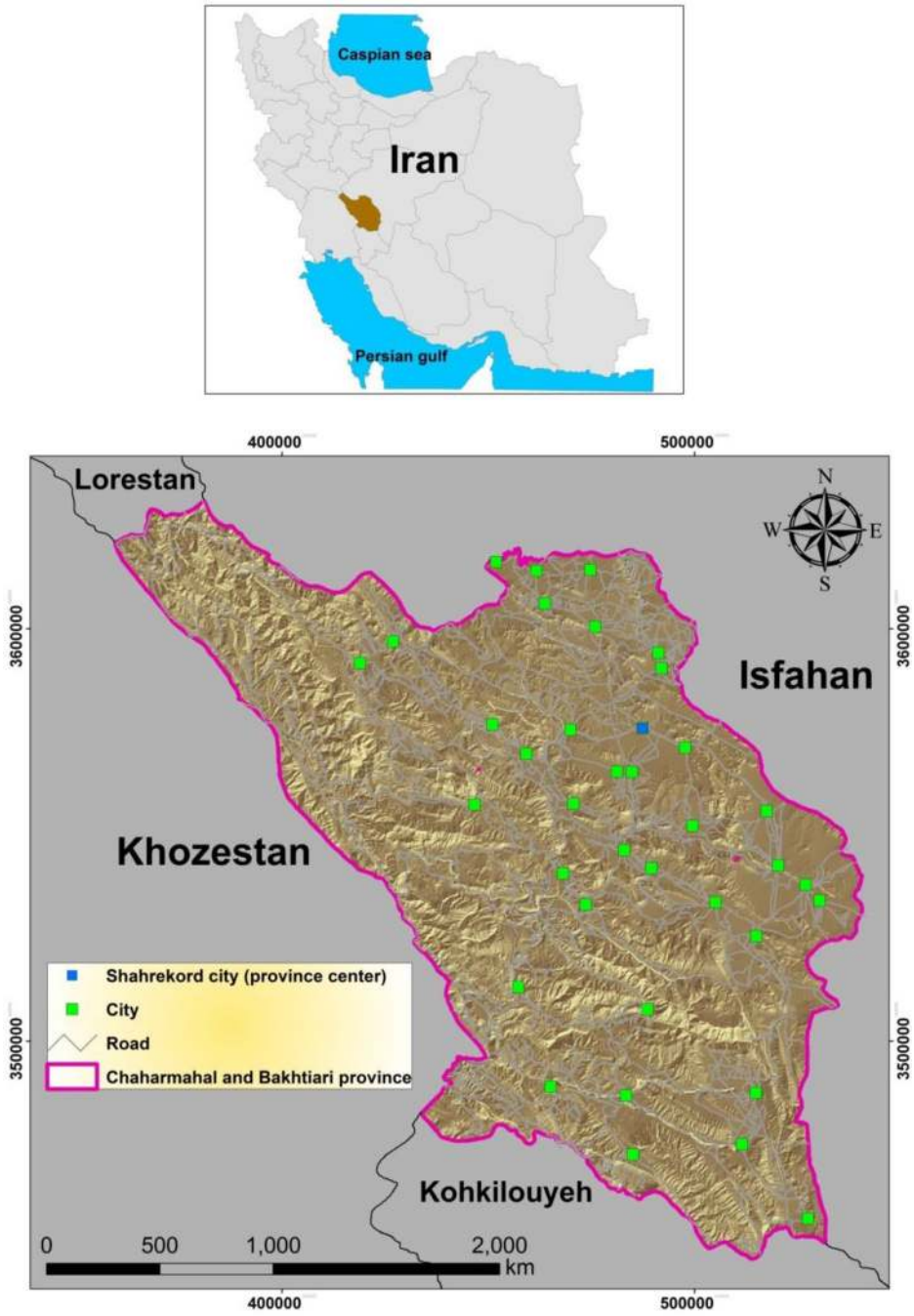

Figure 1. Location of the study area of Chaharmahal and Bakhtiari Province, Iran.

from 28 meteorological stations, digital stream layers, and 895 piezometric wells. These data were obtained from the Regional Water Company of Chaharmahal and Bakhtiari. The social factors were extracted from road networks and residential areas mapped on 1:25,000 topographic maps. The vegetation factors were discerned from Landsat 8 OLI images from June 2018. In addition, to evaluation of the importance of the effective factors for each hazard, specific factors were selected for modeling specific hazards: 12 for wildfires, 8 for snow avalanches, 12 for landslides, 12 for land subsidence, and 12 for floods.

Application of machine learning models. Three state-of-the-art machine learning models were applied in present study to construct the hazard risk maps. Each is explained below.

Functional discriminant analysis (FDA). FDA creates a statistical method to analyze effective factors. It can generally be said that models based on discrimination do unsupervised work so that each class is subdivided into its own subclass; each subclass is given a special value[71,72]. The FDA model is a special combination of regression

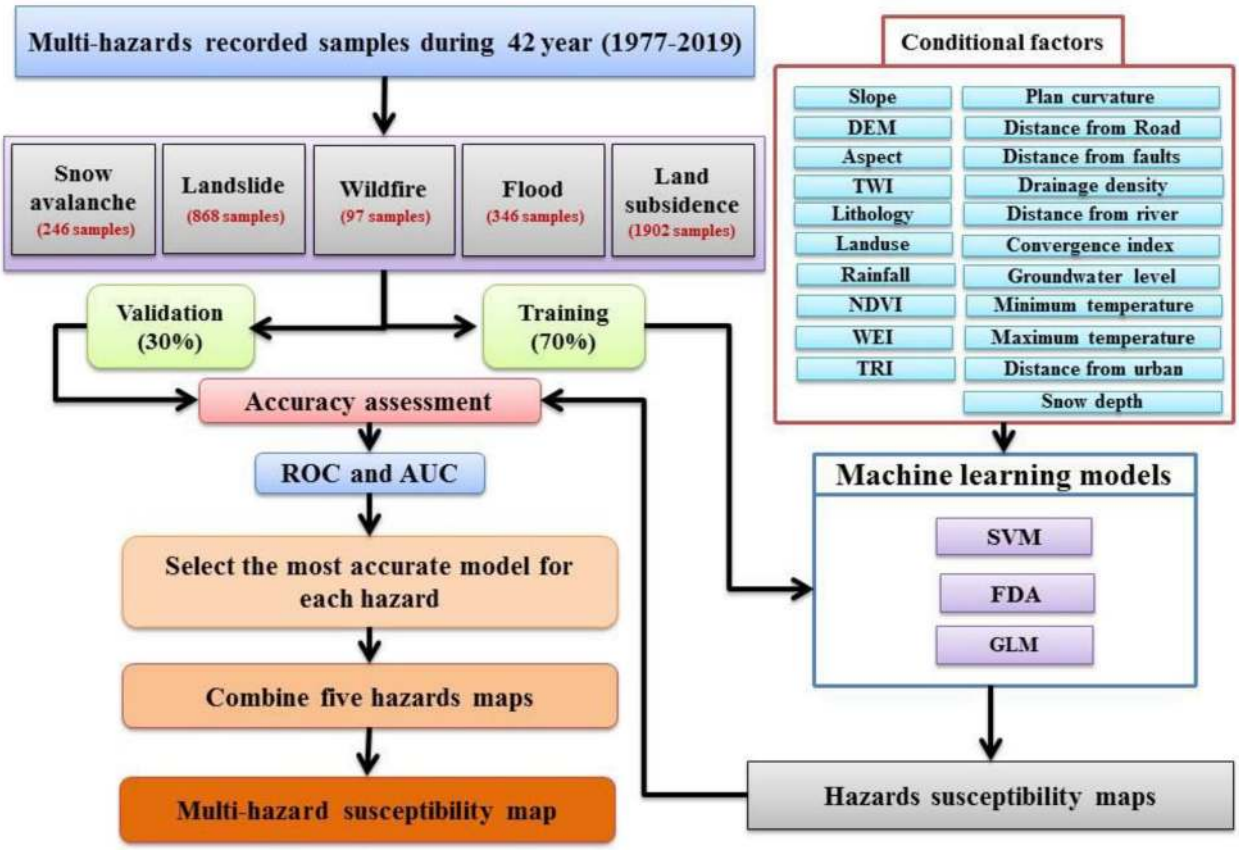

Figure 2. Flowchart of the study methodology.

models that implements a hidden process for each class in the modeling process, especially when conducting complex class modelin[73,74]. The FDA model is similar to other statistical methods, so it can perform just as well[75]. But, since the FDA model is nonparametric, it has been used in a wide range of fields[76]. The FDA model is new to analyses of data, but it has been convenient to use it as a replacement for functions. Therefore, more attention should be paid to this method[77].

Generalized linear model (GLM). The GLM is regression-based so it can reveal differences between variables[78]. The GLM is created from several linear models, and it constructs a best regression model that can predict multiple events[79–81]. Some researchers have reported that GLM is most often used for spatial modeling[55,82–85]. In general, the GLM uses multiple regression to increase accuracy and quality of the results because it can establish a very clear relationship between the dependent and independent variables[86].

Support vector machine (SVM). SVM uses both classification and regression, based on the concept of controlled learning. Results have shown that it generates the smallest clustering errors[87]. Since this model's approach is based on statistical learning theory, it reduces errors and identifies the optimal response[88]. SVM indicates performance estimation by answering a convex optimization problem[89,90]. The SVM model provides a very important advantage: it identifies and analyzes layers effectively[91].

Multi-hazards risk mapping. Snow-avalanche hazard (SAH), landslide hazard (LH), wildfire hazard (WFH), land-subsidence hazard (LSH), and flood hazard (FH) maps were created from the effective factors with the three machine learning models (Fig. 4). First, susceptibility to each hazard was created according to the dependent variables (locations of landslides, floods, avalanches, etc.) and some effective factors (the independent variables) using machine learning techniques. Next, the models with the highest accuracies, determined from ROC-AUC values, were selected and used for multi-hazard mapping. These models were integrated using a Boolean algorithm based on four classes for each hazard—low, moderate, high, and very high. A review of the literature[44,45] indicated that susceptibility classes of low and moderate were low hazard (0) conditions and high and very high were deemed high hazard (1) conditions. To facilitate integration, the four-class maps produced for each hazard by the best models (from among the three algorithms) were reassigned these two classes: 0 and 1. The maps of the five natural events (flood, landslides, land subsidence, snow avalanches, and wildfires) were combined to create an integrated multi-hazard (MH) map (i.e., MH = SAH + LH + LSH + WFH + FH) in ArcGIS and the result was reclassified (Fig. 5).

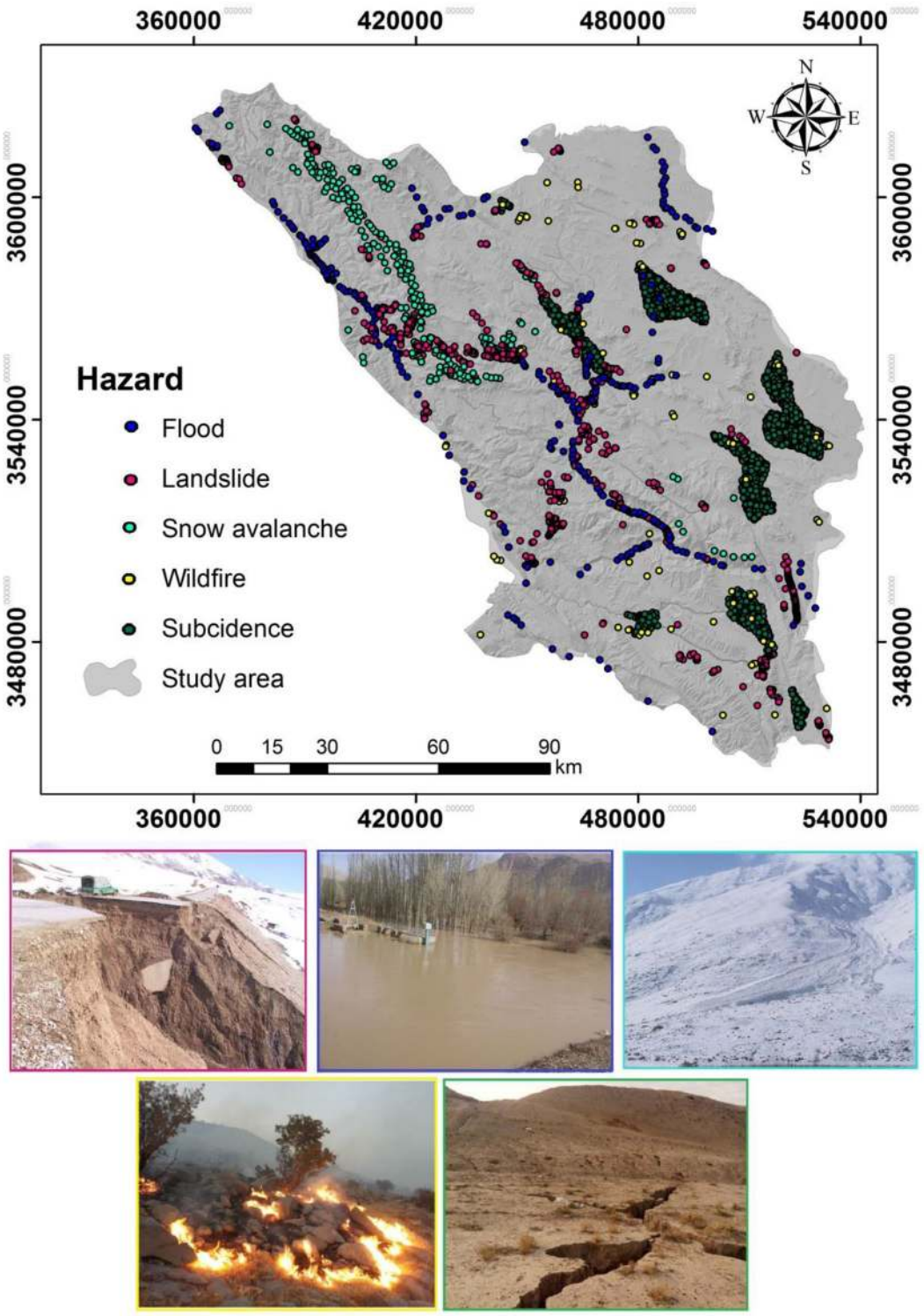

Figure 3. Distribution of the occurrence of the five hazards between 1977 and 2019 in Chaharmahal and Bakhtiari Province (**a**), and images of the five natural extreme events in the study area (**b**) taken by Saleh Yousefi (First author).

Accuracy assessment. The accuracy of each of the MH maps was assessed with the training group data (for the goodness-of-fit test) and the validation group data (for the predictive-performance test) using area under the curve (AUC). AUC is a scalar measure that is a threshold-independent method[92,93]. An area of 1 represents perfect classification, while an area of 0.5 or less indicates poor classification of locations by a model[45,94–96]. In the present study, to produce multi-hazard susceptibility maps of snow avalanches, land subsidence, wildfires,

Effective factors		Hazard				
Full name	Abbreviation	Flood (F)	Wildfire (WF)	Snow avalanche (SA)	Landslide (L)	Land subsidence (LSu)
Rainfall	R	*	*			
Digital elevation model	DEM	*	*	*	*	*
Land use	LU	*		*	*	*
Lithology	Lit	*			*	*
Fault distance	FD				*	*
Slope	S	*	*	*	*	*
River distance	RD	*	*		*	*
Groundwater level	GL					*
Normalized difference vegetation index	NDVI	*	*			*
Road distance	RoD	*	*		*	*
Topographic wetness index	TWI	*	*		*	*
Plan curvature	PC	*		*	*	*
Aspect	A	*	*	*	*	*
Drainage density	DD	*			*	
Convergence Index	CI				*	
Minimum temperature	MinT		*			
Maximum temperature	MaxT		*			
Urban area distance	UD		*			
Wind exposition index	WEI		*	*		
Terrain ruggedness index	TRI			*		
Snow depth	SD			*		

Table 1. The effective factors for susceptibility mapping of five hazards.

landslides, and flood by GLM, FDA, and SVM models a special package was applied in the R software version R 3.5.3. The packages used were "svm"[60,97], "glm"[55,63], and "fda"[17,66].

Results

Accuracy assessments of the hazard maps using AUC. Assessing the accuracies of the three machine learning models (Table 2) demonstrated that FDA (for SAH), SVM (LSH), GLM (WH), SVM (LH), and SVM (FH) provided the most accurate models. The values of AUC these five models were all greater than 0.8, indicating strong classification success and confirmed that the models were acceptably accurate.

Integrated multi-hazard (MH) map. The results of the MH map show that the hazards do not overlap (Table 3 and Fig. 5). More than 1/6th (16.51%) of the province is free of all five hazards. Five sixths (83.49%) of Chaharmahal and Bakhtiari Province experiences at least one of the hazards.

Discussion

Arid and semi-arid regions of the world experience extreme natural events that threaten the structures and daily functions of localities[98]. Natural hazards can cause a great deal of economic damages[99], interruptions, injuries, and loss of life. Mountainous regions are among the most disaster-prone parts of the world because of their geological, climatological, and hydrological characteristics[100,101].

An effective way to begin to manage natural disasters is to map hazards. The information generated can be very useful for effective planning and management of people and activities. Most natural hazards studies have focused on single hazards. Single-hazard approaches focus on hazards as independent phenomena, ignoring the domain of relationships between the hazards[32] and this may lead to miscalculations of risk[102–107]. A greater emphasis on the interactions between and combinations of hazards' risks is needed[102]. Studies that have focused on multi-hazard approaches have concluded that there is collectively greater risk from the interactions of multiple hazards than is yielded by simply combining the results of single-hazard studies. The increasing use of GIS in natural resources management and the introduction of various algebraic, statistical, and empirical methods have enabled better assessments of natural hazards. The methods have been developed in different parts of the world based on different conditions and with different amounts of available data, but they have advanced the modeling process and have revealed the spatial distributions of the natural hazards in many study areas.

Several methods have been used to model and map different natural hazards. For example, flood risk has been assessed using support vector machine (SVM), frequency ratio (FR), multivariate statistical analysis, weight of evidence (WoE), analytic hierarchy process (AHP), and decision trees (DTs). The analytic hierarchy process (AHP) method is one of the most common ways to solve problems associated with the use of multiple

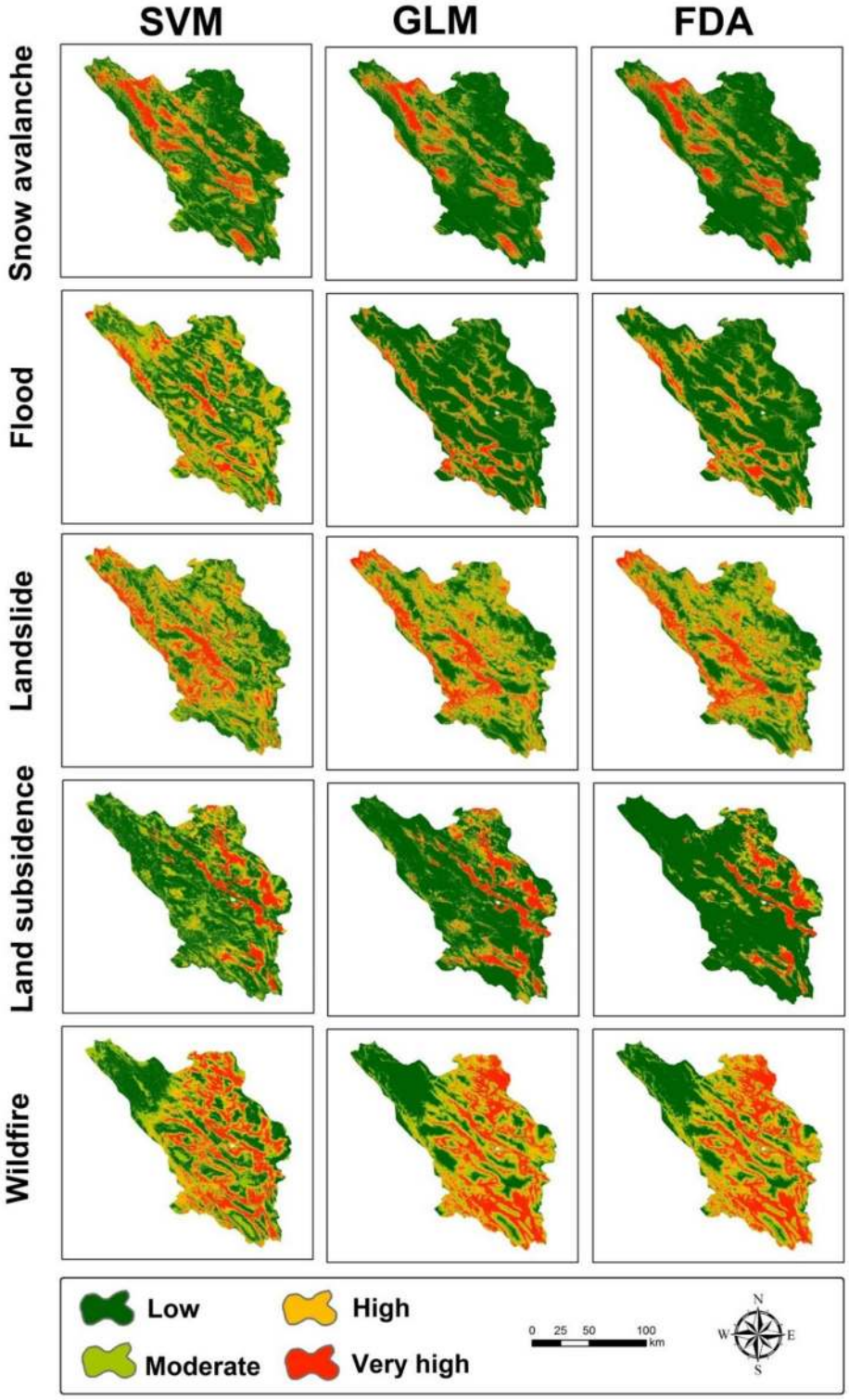

Figure 4. The risk maps of the five hazards created from the three machine learning models for Chahaharmahal and Bakhtiari Province.

variables[108,109] and it is often used in hazard assessments[110]. However, mapping processes are very sensitive to changes in expert's judgments and to changes in weighting the input variables at the assessment scale and are significant disadvantages[109]. The most popular methods used in landslide risk assessments are neuro-fuzzy inference systems[111], logistic regression models, analytic hierarchy process, statistical indices[112], vector based methods[113], and artificial neural networks[114]. For wildfire risk assessment, probabilistic models and maximum entropy models[115,116], neural network (NN)[117–119], fuzzy logic [120–122], logistic regression (LR)[21,123–125], decision

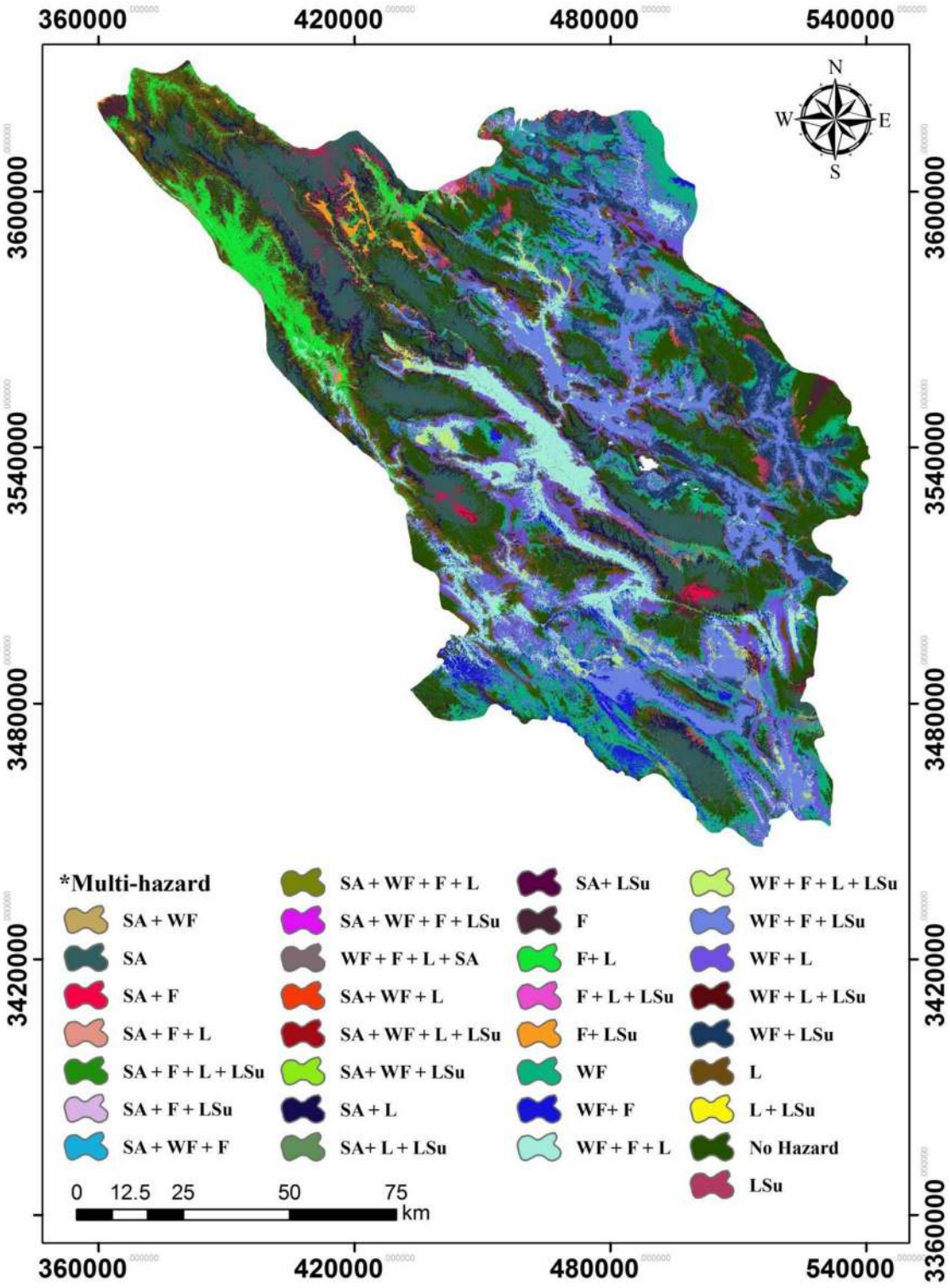

Figure 5. The multi-hazard risk map based on a combination of the five best hazard risk maps for Chaharmahal and Bakhtiari Province (**L* Landslide, *L*Su Land subsidence, *F* Flood, *WF* Wildfire, *SA* Snow avalanche).

tree (DT)[126], the random forest (RF)[127–129], and support vector machine (SVM)[24,130] have been used. Numerous methods have also been used for mapping snow avalanche risk: multi-criteria decision making approaches[131–133], fuzzy–frequency ratio models[134–136], numerical methods, dynamic models[137], and remote sensing-based methods[138,139]. Though remote sensing can provide useful information about snow avalanches, the complex relationships between snow avalanches and geomorphometric variables are often overlooked, and most risk assessments are based on expert opinion. And prediction of land subsidence risk has used methods like artificial neural networks[140], frequency ratio[141], logistic regression[142], and differential radar interferometry[143].

Model	Hazard				
	Flood (F)	Wildfire (WF)	Snow avalanche (SA)	Landslide (L)	Land subsidence (LSu)
SVM	**0.975**	0.835	0.894	**0.841**	**0.943**
FDA	0.962	0.825	**0.912**	0.779	0.920
GLM	0.965	**0.837**	0.909	0.777	0.923

Table 2. AUC values for three machine learning models in mapping natural hazards.

Multi-hazard	Area (ha)	Percent (%)
No hazard	269,093.34	16.511
SA	186,049.44	11.416
WF	180,470.97	11.074
WF + L	160,292.88	9.835
WF + F + LSu	136,861.83	8.398
L	133,069.95	8.165
WF + F + L	114,211.8	7.008
WF + LSu	101,536.92	6.230
SA + L	84,893.76	5.209
F + L	65,183.67	4.000
WF + F	55,212.84	3.388
F	45,086.31	2.766
WF + F + L + LSu	22,783.14	1.398
LSu	15,398.73	0.945
WF + L + LSu	12,496.86	0.767
SA + F	12,462.66	0.765
F + LSu	10,308.87	0.633
SA + F + L	7,746.75	0.475
SA + WF + L	6,630.3	0.407
SA + WF	3,918.69	0.240
F + L + LSu	2,751.12	0.169
L + LSu	1,112.31	0.068
SA + WF + F + L	1,084.86	0.067
SA + WF + F	353.25	0.022
SA + F + LSu	273.78	0.017
SA + F + L + LSu	140.67	0.009
SA + LSu	118.53	0.007
SA + WF + F + L	85.77	0.005
SA + L + LSu	48.51	0.003
SA + WF + L + LSu	27.72	0.002
SA + WF + LSu	21.78	0.001

Table 3. Areas of different classes of various hazards.

Machine learning is another modeling technique that is increasingly used to understand the complex relationships between a wide range of independent variables like meteorological factors (winds, air pressure, storm surge, and floods) and a dependent variable[144]. Therefore, these algorithms can aid forecasting of multiple hazards simultaneously, where the environmental conditions vary considerably across a landscape[145].

In this study, we assessed five hazards in a mountainous region of Iran. To comprehensively assess extreme natural events in the study area, multi-hazard mapping was conducted using three machine learning models. Evaluation of the accuracies of the SVM, GLM and FDA models showed that SVM is most accurate when predicting landslide, land subsidence, and flood risks. GLM is most accurate for wildfire risk. And FDA is most accurate for snow-avalanche risk prediciton (Table 2). The AUCs of the five best models were over 0.8, validating their strong performances[146] and demonstrating that they (more or less) accurately predicted the patterns of the hazards in the study area. The SVM method also produced very good results for mapping landslide, land subsidence, and flood risks. Li et al.[147] applied SVM with univariate and multivariate statistical methods to investigate land subsidence. Their results showed that SVM is more accurate than other algorithms they tested. Others have confirmed the high performance of SVM for similar purposes[24,131,148,149]. Studies of landslide risk have also revealed that highly accurate predictions were made with SVM[112,150]. The strong capacity of SVM to

predict flood risk has also been demonstrated[151–153]. GLM has been used to predict wildfire risk[123,154–158]. GLMs have proven to acceptably predict wildfire risks in California[155,159] and Spain[156,160].

The MH risk map was developed by combining the results produced by the SVM, GLM and FDA approaches. Results demonstrate that using the best machine learning models to predict several hazards yields useful information about their interactions. Multi-hazard relationships are very dependent upon the scale of analysis and the specific sets of hazards. Understanding the relationships and interactions between multiple hazards is an important challenge[103]. This study begins to fill this gap. The results show that all five hazards are absent from 16.5% of the study area. The rest of the study area, 83.5%, is likely to be impacted by at least one of the hazards, however. Pourghasemi et al.[54] mapped both the individual and collective risks posed by three hazards (floods, forest fires, and landslides) in a multi-hazard study using machine learning techniques. Others have conducted multi-hazard risk assessments, but separately for each risk[46,47,161].

Conclusions

As mountainous areas are challenged with a wide array of natural hazards and sites within them are prone to exposures to multiple natural hazards, this study evaluated the spatial distribution of risk from multiple hazards in Chaharmahal and Bakhtiari Province, Iran, using three machine learning models (SVM, GLM and FDA). Identification of high-risk areas is the most important issue for most decision makers and natural resource managers. In this regard, we presented a multi-hazard risk map for five natural hazards (floods, landslides, land subsidence, snow avalanches, and forest fires) in the study area. Evaluation of the accuracies of the maps produced by the SVM, GLM, and FDA models showed that SVM is most accurate model for predicting landslide, land subsidence, and flood risks. GLM is best for wildfire risk prediction. And FDA is best for snow avalanche risk assessment in the region. The results indicate that 16.5% of the study area is not likely to experience any of the five natural hazards, but the rest of province (83.5%) is at risk from exposure to at least one of the five (or several or perhaps all): 11.41% is possesses snow avalanche risk, 11.07% wildfire risk, and 9.83% landslide risk. Each type of machine learning method achieved acceptable levels of accuracy in their predictions. Therefore, these results can be regarded with high confidence and may be used in future studies to examine the spatial distributions of risks from multiple hazards and to provide useful information for proactive management and hazard mitigation.

Received: 12 April 2020; Accepted: 9 July 2020
Published online: 22 July 2020

References

1. Fuchs, S., Keiler, M. & Zischg, A. A spatiotemporal multi-hazard exposure assessment based on property data. *Nat. Hazard. Earth Syst. Sci.* **15**, 2127–2142 (2015).
2. Barthel, F. & Neumayer, E. A trend analysis of normalized insured damage from natural disasters. *Clim. Chang.* **113**, 215–237 (2012).
3. Munich, R. E., Kron, W. & Schuck, A. *Topics geo: natural catastrophes 2013: analyses, assessments, positions* (Munchener Ruckversicherungs-Gesellschaft, Munich, 2014).
4. Guzzetti, F., Carrara, A., Cardinali, M. & Reichenbach, P. Landslide hazard evaluation: a review of current techniques and their application in a multi-scale study, Central Italy. *Geomorphology* **31**, 181–216 (1999).
5. Guzzetti, F., Reichenbach, P., Cardinali, M., Galli, M. & Ardizzone, F. Probabilistic landslide hazard assessment at the basin scale. *Geomorphology* **72**(1–4), 272–299 (2005).
6. Varnes, D. Slope movement types and processes. In *Landslides: Analysis and Control* (eds Schuster, R. L. & Krizek, R. J.) (Transportation Research Board, National Academy of Science, Washington, 1978).
7. Bell, R. & Glade, T. Multi-hazard analysis in natural risk assessments. *WIT Trans. Ecol. Environ.* **77**, 1–10 (2004).
8. Jamieson, B. & Stethem, C. Snow avalanche hazards and management in Canada: challenges and progress. *Nat. Hazards* **26**, 35–53 (2002).
9. Meseşan, F., Man, T. C., Pop, O. T. & Gavrilă, I. G. Reconstructing snow-avalanche extent using remote sensing and dendrogeomorphology in Parâng Mountains. *Cold Reg. Sci. Technol.* **157**, 97–109 (2019).
10. Suresh, D., Yarrakula, K., Venkateswarlu, B., Mohanty, B., & Manupati, V. Risk mapping analysis with geographic information systems for landslides using supply chain. In *Emerging Applications in Supply Chains for Sustainable Business Development*. 131–141 (IGI Global, 2019).
11. Barredo, J. I. Major flood disasters in Europe: 1950–2005. *Nat. Hazards* **42**, 125–148 (2007).
12. Rahmati, O., Zeinivand, H. & Besharat, M. Flood hazard zoning in Yasooj region, Iran, using GIS and multi-criteria decision analysis. *Geom. Nat. Hazards Risk* **1**, 1–18 (2015).
13. Tsereteli, E., Gaprindashvili, G., Gaprindashvili, M., Bolashvili, N., & Gongadze, M. Hazard risk of debris/mud flow events in Georgia and methodological approaches for management. *IAEG/AEG Annual Meeting Proceedings, San Francisco, California, 2018-Volume 5*. 153–160 (Springer, New York, 2019).
14. Corona, C. & Stoffel, M. Snow & ice avalanches. *Int. Encycl. Geogr.* **10**, 1–7 (2016).
15. Pardini, G., Gispert, M. & Dunjó, G. Runoff erosion and nutrient depletion in five Mediterranean soils of NE Spain under different land use. *Sci. Total Environ.* **309**, 213–224 (2003).
16. Prosdocimi, M., Cerdà, A. & Tarolli, P. Soil water erosion on Mediterranean vineyards: a review. *CATENA* **141**, 1–21 (2016).
17. Gayen, A., & Pourghasemi, H. R. Spatial modeling of gully erosion: a new ensemble of CART and GLM data-mining algorithms. In *Spatial Modeling in GIS and R for Earth and Environmental Sciences*, 653–669 (Elsevier, Amsterdam, 2019). https://doi.org/10.1016/B978-0-12-815226-3.00030-2.
18. Michoud, C. *et al.* Rockfall hazard and risk assessments along roads at a regional scale: example in Swiss Alps. *Nat. Hazards Earth Syst. Sci.* **12**, 3 (2012).
19. Page, Y. L. *et al.* Global fire activity patterns (1996–2006) and climatic influence: an analysis using the World Fire Atlas. *Atmos. Chem. Phys.* **8**, 1911–1924 (2008).
20. Abatzoglou, J. T. & Kolden, C. A. Relationships between climate and macro scale area burned in the western United States. *Int. J. Wildl. Fire* **22**, 1003–1020 (2013).
21. Eskandari, S. & Chuvieco, E. Fire danger assessment in Iran based on geospatial information. *Int. J. Appl. Earth Obs. Geoinf.* **42**, 57–64 (2015).

22. Pourghasemi, H. R. GIS-based forest fire susceptibility mapping in Iran: a comparison between evidential belief function and binary logistic regression models. *Scand. J. For. Res.* **31**(1), 80–98 (2016).
23. Pourtaghi, Z. S., Pourghasemi, H. R., Aretano, R. & Semeraro, T. Investigation of general indicators influencing on forest fire and its susceptibility modeling using different data mining techniques. *Ecol. Ind.* **64**, 72–84 (2016).
24. Gigovic, L., Pourghasemi, H. R., Drobnjak, S. & Bai, Sh. Testing a new ensemble model based on SVM and random forest in forest fire susceptibility assessment and its mapping in Serbia's Tara. *Forests* **10**, 408 (2019).
25. Haigh, M. J., Rawat, J. S., Rawat, M. S., Bartarya, S. K. & Rai, S. P. Interactions between forest and landslide activity along new highways int he Kumaun Himalaya. *For. Ecol. Manage.* **78**, 173–189 (1995).
26. Spitz, W., Lagasse, P., Schumm, S., & Zevenbergen, L. A Methodology for Predicting Channel Migration NCHRP Project No. 24–16 (2001). *Nchrp*. DOI: 10.1061/40581(2001)106.
27. Hand, W. H., Fox, N. I. & Collier, C. G. A study of twentieth-century extreme rainfall events in the United Kingdom with implications for forecasting. *Meteorol. Appl.* **11**, 15–31 (2004).
28. Amiri, M. J. & Eslamian, S. S. Investigation of climate change in Iran. *J. Environ. Sci. Technol.* **3**, 208–216 (2010).
29. Pourghasemi, H. R., Yousefi, S., Kornejady, A. & Cerdà, A. Performance assessment of individual and ensemble data-mining techniques for gully erosion modeling. *Sci. Total Environ.* **609**, 764–775 (2017).
30. Rijsdijk, A., Sampurno Bruijnzeel, L. A. & Sutoto, C. K. Runoff and sediment yield from rural roads, trails and settlements in the upper Konto catchment, East Java, Indonesia. *Geomorphology* **87**, 28–37 (2007).
31. Finlay, P. J. & Fell, R. Landslides: risk perception and acceptance. *Can. Geotech. J.* **34**, 169–188 (1997).
32. Kappes, M. S., Keiler, M., von Elverfeldt, K. & Glade, T. Challenges of analyzing multi-hazard risk: a review. *Nat. Hazards* **64**, 1925–1958 (2012).
33. Hungr, O., Evans, S. G. & Hazzard, J. Magnitude and frequency of rock falls and rock slides along the main transportation corridors of southwestern British Columbia. *Can. Geotech. J.* **36**, 224–238 (1999).
34. Statham, G. *et al.* A conceptual model of avalanche hazard. *Nat. Hazards* **90**, 663–691 (2018).
35. Barbolini, M., Pagliardi, M., Ferro, F. & Corradeghini, P. Avalanche hazard mapping over large undocumented areas. *Nat. Hazards* **56**, 451–464 (2011).
36. McClung, D. & Schaerer, P. A. *The Avalanche Handbook* (The Mountaineers Books, Vancouver, 2006).
37. Van Westen, C., Alkema, D., Damen, M. C. J., Kerle, N., & Kingma, N. C. Multi-hazard risk assessment. *Distance education course. Guide book. United Nations University–ITC School on Disaster Geoinformation Management (UNUITC DGIM).[En línea]. Disponible en:* ftp://ftp.itc.nl/pub/westen/Multi_hazardrisk_course/Guidebook/Guidebook%2520MHRA.pdf. *Fecha de con* **25** (2011).
38. Stethem, C. *et al.* Snow avalanche hazard in Canada: a review. *Nat. Hazards* **28**, 487–515 (2003).
39. Christophe, C., Georges, R., Jérôme, L. S., Markus, S. & Pascal, P. Spatio-temporal reconstruction of snow avalanche activity using tree rings: Pierres Jean Jeanne avalanche talus, Massif de l'Oisans, France. *CATENA* **83**, 107–118 (2010).
40. Bühler, Y., Christen, M., Kowalski, J. & Bartelt, P. Sensitivity of snow avalanche simulations to digital elevation model quality and resolution. *Ann. Glaciol.* **52**, 72–80 (2011).
41. Demirkesen, A. C. Multi-risk interpretation of natural hazards for settlements of the Hatay province in the east Mediterranean region, Turkey using SRTM DEM. *Environ. Earth Sci.* **65**, 1895–1907 (2012).
42. Germain, D. Snow avalanche hazard assessment and risk management in northern Quebec, eastern Canada. *Nat. Hazards* **80**, 1303–1321 (2016).
43. Clark, T. *Exploring the Link Between the Conceptual Model of Avalanche Hazard and the North American Public Avalanche Danger Scale* (SIMON FRASER UNIVERSITY, Burnaby, 2019).
44. Pourghasemi, H. R., Gayen, A., Panahi, M., Rezaie, F. & Blaschke, T. Multi-hazard probability assessment and mapping in Iran. *Sci. Total Environ.* **692**, 556–571. https://doi.org/10.1016/j.scitotenv.2019.07.203 (2019).
45. Pourghasemi, H. R. *et al.* Assessing and mapping multi-hazard risk susceptibility using a machine learning technique. *Sci. Rep.* **10**, 1–11 (2020).
46. Schmidt, J. *et al.* Quantitative multi-risk analysis for natural hazards: a framework for multi-risk modelling. *Nat. Hazards* **58**, 1169–1192 (2011).
47. Gruber, F. E. & Mergili, M. Regional-scale analysis of high-mountain multi-hazard and risk indicators in the Pamir (Tajikistan) with GRASS GIS. *Nat. Hazards Earth Syst. Sci.* **13**, 2779–2796 (2013).
48. Bahrainy, H. Natural disaster management in Iran during the 1990s—need for a new structure. *J. Urban Plan. Dev.* **129**, 140–160 (2003).
49. Rahmati, O., Tahmasebipour, N., Haghizadeh, A., Pourghasemi, H. R. & Feizizadeh, B. Evaluating the influence of geo-environmental factors on gully erosion in a semi-arid region of Iran: an integrated framework. *Sci. Total Environ.* **579**, 913–927 (2017).
50. Yousefi, S. *et al.* Effects of urbanization on river morphology of the Talar River, Mazandarn Province, Iran. *Geocarto Int.* **1**, 1–17 (2017).
51. Shahabi, H. & Ahmad, B. Application of MODIS image satellite and GIS technique in assessment of avalanche fall in roads. *Proc. World Acad. Sci. Eng. Technol.* **57**, 713–717 (2011).
52. Tabari, H., Abghari, H., Hosseinzadeh, H. & Talaee, P. Temporal trends and spatial characteristics of drought and rainfall in arid and semiarid regions of Iran. *Hydrol. Process.* **26**, 3351–3361 (2012).
53. Mirzaee, S. *et al.* Effects of hydrological events on morphological evolution of a fluvial system. *J. Hydrol.* **563**, 33–42 (2018).
54. Pourghasemi, H. R., Gayen, A., Edalat, M., Zarafshar, M. & Tiefenbacher, J. P. Is multi-hazard mapping effective in assessing natural hazards and integrated watershed management?. *Geosci. Front.* **11**, 1203–1217 (2019).
55. Ghanbarian, G., Raoufat, M.R., Pourghasemi, H.R., & Safaeian, R. Habitat Suitability Mapping of Artemisia aucheri Boiss Based on the GLM Model in R. *Spatial Modeling in GIS and R for Earth and Environmental Sciences*. 213–227 (Elsevier, Amsterdam, 2019). DOI: 10.1016/b978-0-12-815226-3.00009-0.
56. Marmion, M., Hjort, J., Thuiller, W. & Luoto, M. A comparison of predictive methods in modelling the distribution of periglacial landforms in Finnish Lapland. *Earth Surf. Proc. Land.* **33**(14), 2241–2254 (2008).
57. Vilar, L. *et al.* Multitemporal modelling of socio-economic wildfire drivers in central Spain between the 1980s and the 2000s: comparing generalized linear models to machine learning algorithms. *PLoS ONE* **11**(8), e0161344 (2016).
58. Rahmati, O., Pourghasemi, H. R. & Melesse, A. M. Application of GIS-based data driven random forest and maximum entropy models for groundwater potential mapping: a case study at Mehran Region, Iran. *CATENA* **137**, 360–372 (2016).
59. Zhang, L. *et al.* Classification and regression with random forests as a standard method for presence-only data SDMs: a future conservation example using China tree species. *Ecol. Inform.* **52**, 46–56 (2019).
60. Abdollahi, S., Pourghasemi, H. R., Ghanbarian, G. A. & Safaeian, R. Prioritization of effective factors in the occurrence of land subsidence and its susceptibility mapping using an SVM model and their different kernel functions. *Bull. Eng. Geol. Environ.* **78**(6), 4017–4034 (2019).
61. Rahimian Boogar, A., Salehi, H., Pourghasemi, H. R. & Blaschke, T. Predicting habitat suitability and conserving *Juniperus* spp. habitat using SVM and maximum entropy machine learning techniques. *Water* **11**(10), 2049 (2019).
62. Marjanović, M., Kovačević, M., Bajat, B. & Voženílek, V. Landslide susceptibility assessment using SVM machine learning algorithm. *Eng. Geol.* **123**(3), 225–234 (2011).

63. Naghibi, S. A. & Pourghasemi, H. R. A comparative assessment between three machine learning models and their performance comparison by bivariate and multivariate statistical methods in groundwater potential mapping. *Water Resour. Manage* **29**(14), 5217–5236 (2015).
64. Rahmati, O. *et al.* Multi-hazard exposure mapping using machine learning techniques: a case study from Iran. *Remote Sens.* **11**(16), 1943 (2019).
65. Rodrigues, M. & de la Riva, J. An insight into machine-learning algorithms to model human-caused wildfire occurrence. *Environ. Model. Softw.* **57**, 192–201 (2014).
66. Hosseinalizadeh, M. *et al.* Spatial modelling of gully headcuts using UAV data and four best-first decision classifier ensembles (BFTree, Bag-BFTree, RS-BFTree, and RF-BFTree). *Geomorphology* **349**, 184–193 (2019).
67. Bednarik, M., Magulová, B., Matys, M. & Marschalko, M. Landslide susceptibility assessment of the Kraľovany-Liptovský Mikuláš railway case study. *Phys. Chem. Earth A/B/C* **35**(3–5), 162–171 (2010).
68. Ruppert, D. The elements of statistical learning: data mining, inference, and prediction. *J. Am. Stat. Assoc.* https://doi.org/10.1198/jasa.2004.s339 (2004).
69. Haghighian, F., Yousefi, S. & Keesstra, S. Identifying tree health using sentinel-2 images: a case study on *Tortrix viridana* L. infected oak trees in Western Iran. *Geocarto Int.* **1**, 1–11 (2020).
70. Hong, H., Naghibi, S. A., Moradi Dashtpagerdi, M., Pourghasemi, H. R. & Chen, W. A comparative assessment between linear and quadratic discriminant analyses (LDA-QDA) with frequency ratio and weights-of-evidence models for forest fire susceptibility mapping in China. *Arab. J. Geosci.* **10**(7), 167 (2017).
71. Chamroukhi, F., Glotin, H., & Rabouy, C. Functional mixture discriminant analysis with hidden process regression for curve classification. *ESANN 2012 Proceedings, 20th European Symposium on Artificial Neural Networks, Computational Intelligence and Machine Learning* 281–286 (2012).
72. Zou, M. *et al.* Fisher discriminant analysis for classification of autism spectrum disorders based on folate-related metabolism markers. *J. Nutr. Biochem.* **64**, 25–31 (2019).
73. Gui, J., & Li, H. Mixture Functional Discriminant Analysis for Gene Function Classification Based on Time Course Gene Expression Data. *Proceeding Joint Statistical Meeting (Biometrics Section)* (2003).
74. Ray, A., Dhir, A., Bala, P. K. & Kaur, P. Why do people use food delivery apps (FDA)? A uses and gratification theory perspective. *J. Retail. Consum. Serv.* **51**, 221–230 (2019).
75. Nikitović, V. Functional data analysis in forecasting Serbian fertility. *Stanovnistvo* **49**, 73–89 (2011).
76. Lu, Z. Q. J. Nonparametric functional data analysis: theory and practice. *Technometrics* https://doi.org/10.1198/tech.2007.s483 (2007).
77. Auton, T. Applied functional data analysis: methods and case studies. *J. R. Stat. Soc. A* https://doi.org/10.1111/j.1467-985x.2004.t01-5-.x (2004).
78. Ozdemir, A. & Altural, T. A comparative study of frequency ratio, weights of evidence and logistic regression methods for landslide susceptibility mapping: Sultan mountains, SW Turkey. *J. Asian Earth Sci.* **64**, 180–197 (2013).
79. Federici, P. R. *et al.* Multidisciplinary investigations in evaluating landslide susceptibility: an example in the Serchio River valley (Italy). *Quatern. Int.* **171–172**, 52–63 (2007).
80. Greco, R., Sorriso-Valvo, M. & Catalano, E. Logistic regression analysis in the evaluation of mass movements susceptibility: the aspromonte case study, Calabria, Italy. *Eng. Geol.* **89**, 47–66 (2007).
81. Payne, R. *A Guide to Regression, Nonlinear and Generalized Linear Models in Genstat* 18th edn. (VSN International, Hemel Hempstead, 2015).
82. Guisan, A. & Zimmermann, N. E. Predictive habitat distribution models in ecology. *Ecol. Model.* **135**, 147–186 (2000).
83. Bolker, B. M. *et al.* Generalized linear mixed models: a practical guide for ecology and evolution. *Trends Ecol. Evol.* **24**, 127–135 (2009).
84. Rupprecht, F., Oldeland, J. & Finckh, M. Modelling potential distribution of the threatened tree species *Juniperus oxycedrus*: how to evaluate the predictions of different modelling approaches?. *J. Veg. Sci.* **22**, 647–659 (2011).
85. Dumbser, M., Fambri, F., Gaburro, E. & Reinarz, A. On GLM curl cleaning for a first order reduction of the CCZ4 formulation of the Einstein field equations. *J. Comput. Phys.* **404**, 109088 (2020).
86. Scott, A. J., Hosmer, D. W. & Lemeshow, S. Applied logistic regression. *Biometrics* **47**, 1632 (1991).
87. Amiri, M., Pourghasemi, H. R., Ghanbarian, G. A. & Afzali, S. F. Assessment of the importance of gully erosion effective factors using Boruta algorithm and its spatial modeling and mapping using three machine learning algorithms. *Geoderma* **340**, 55–69 (2019).
88. Vapnik, V., Guyon, I. & Hastie, T. Support vector machines. *Mach. Learn.* **20**, 273–297 (1995).
89. Nansen, C. & Elliott, N. Remote sensing and reflectance profiling in entomology. *Annu. Rev. Entomol.* https://doi.org/10.1146/annurev-ento-010715-023834 (2016).
90. Yousefi, S. *et al.* Accuracy assessment of land cover/land use classifiers in dry and humid areas of Iran. *Environ. Monit. Assess.* **187**, 641 (2015).
91. Micheletti, N., Foresti, L., Kanevski, M., Pedrazzini, A., & Jaboyedoff, M. Landslide susceptibility mapping using adaptive support vector machines and feature selection. Master Thesis submitted to University of Lausanne Faculty of Geosciences and Environment for the Degree of Master of Science in Environmental Geosciences (2011).
92. Hanley, J. A. & McNeil, B. J. The meaning and use of the area under a receiver operating characteristic (ROC) curve. *Radiology* **143**, 29–36 (1982).
93. Marzban, C. The ROC curve and the area under it as performance measures. *Weather Forecast.* **19**, 1106–1114 (2004).
94. Yesilnacar, E. K. The application of computational intelligence to landslide susceptibility mapping in Turkey. Ph.D. Thesis, Department of Geomatics, University of Melbourne, Melbourne, (2005).
95. Youssef, A. M., Pourghasemi, H. R., Pourtaghi, Z. S. & Al-Katheeri, M. M. Landslide susceptibility mapping using random forest, boosted regression tree, classification and regression tree, and general linear models and comparison of their performance at Wadi Tayyah Basin, Asir Region, Saudi Arabia. *Landslides* **13**, 839–856 (2016).
96. Golkarian, A., Naghibi, S. A., Kalantar, B. & Pradhan, B. Groundwater potential mapping using C50, random forest, and multivariate adaptive regression spline models in GIS. *Environ. Monit. Assess.* **190**(3), 149 (2018).
97. Pouteau, R., Meyer, J.-Y., Taputuarai, R. & Stoll, B. Support vector machines to map rare and endangered native plants in Pacific islands forests. *Ecol. Inform.* **9**, 37–46 (2012).
98. Cerdà, A. & Robichaud, P. R. *Fire effects on soil infiltration. Fire effects on soil and restoration strategies* 97–120 (CRC Press, Boca Raton, 2009).
99. Aleotti, P. & Chowdhury, R. Landslide hazard assessment: summary review and new perspectives. *Bull. Eng. Geol. Environ.* **58**, 21–44 (1999).
100. McGuire, K. J. & McDonnell, J. J. Hydrological connectivity of hillslopes and streams: characteristic time scales and nonlinearities. *Water Resour. Res.* **46**, 1–10 (2010).
101. Nikolopoulos, E. I., Anagnostou, E. N., Borga, M., Vivoni, E. R. & Papadopoulos, A. Sensitivity of a mountain basin flash flood to initial wetness condition and rainfall variability. *J. Hydrol.* **402**, 165–178 (2011).
102. Hewitt, K. & Burton, I. The hazardousness of a place: a regional ecology of damaging events. *Research Series* (1971).
103. Kappes, M., Keiler, M. & Glade, T. From single-to multi-hazard risk analyses: a concept addressing emerging challenges (2010).

104. Gill, J. C. & Malamud, B. D. Reviewing and visualizing the interactions of natural hazards. *Rev. Geophys.* **52**, 680–722 (2014).
105. Duncan, M., Edwards, S., Kilburn, C., Twigg, J. & Crowley, K. An interrelated hazards approach to anticipating evolving risk. *Global Facility for Disaster Reduction and Recovery* (2016).
106. Gill, J. C. & Malamud, B. D. Hazard interactions and interaction networks (cascades) within multi-hazard methodologies. *Earth Syst. Dyn.* **7**, 659 (2016).
107. Montz, B. E., Tobin, G. A. & Hagelman, R. R. *Natural Hazards: Explanation and Integration* (Guilford Publications, New York, 2017).
108. Cheng, C. H. Evaluating naval tactical missile systems by fuzzy AHP based on the grade value of membership function. *Eur. J. Oper. Res.* **96**, 343–350 (1997).
109. Chang, N.-B., Parvathinathan, G. & Breeden, J. B. Combining GIS with fuzzy multicriteria decision-making for landfill siting in a fast-growing urban region. *J. Environ. Manage.* **87**, 139–153 (2008).
110. Dai, F., Lee, C. & Zhang, X. GIS-based geo-environmental evaluation for urban land-use planning: a case study. *Eng. Geol.* **61**, 257–271 (2001).
111. Lee, S. Application and verification of fuzzy algebraic operators to landslide susceptibility mapping. *Environ. Geol.* **52**, 615–623 (2007).
112. Pourghasemi, H. R., Moradi, H. & Aghda, S. F. Landslide susceptibility mapping by binary logistic regression, analytical hierarchy process, and statistical index models and assessment of their performances. *Nat. Hazards* **69**, 749–779 (2013).
113. Xu, C., Xu, X., Dai, F. & Saraf, A. K. Comparison of different models for susceptibility mapping of earthquake triggered landslides related with the 2008 Wenchuan earthquake in China. *Comput. Geosci.* **46**, 317–329 (2012).
114. Conforti, M., Pascale, S., Robustelli, G. & Sdao, F. Evaluation of prediction capability of the artificial neural networks for mapping landslide susceptibility in the Turbolo River catchment (northern Calabria, Italy). *CATENA* **113**, 236–250 (2014).
115. Renard, Q., Pélissier, R., Ramesh, B. & Kodandapani, N. Environmental susceptibility model for predicting forest fire occurrence in the Western Ghats of India. *Int. J. Wildl. Fire* **21**, 368–379 (2012).
116. Xu, J. & Kong, F. Adaptive scaled unscented transformation for highly efficient structural reliability analysis by maximum entropy method. *Struct. Saf.* **76**, 123–134 (2019).
117. Vakalis, D., Sarimveis, H., Kiranoudis, C., Alexandridis, A. & Bafas, G. A GIS based operational system for wildland fire crisis management. I Mathematical modelling and simulation. *Appl. Math. Modell.* **28**(4), 389–410 (2004).
118. Vasilakos, C., Kalabokidis, K., Hatzopoulos, J. & Matsinos, I. Identifying wildland fire ignition factors through sensitivity analysis of a neural network. *Nat. Hazards* **50**(1), 125–143 (2009).
119. Satir, O., Berberoglu, S. & Donmez, C. Mapping regional forest fire probability using artificial neural network model in a Mediterranean forest ecosystem. *Geom. Nat. Hazards Risk* **7**(5), 1645–1658 (2016).
120. Vadrevu, K. P., Eaturu, A. & Badarinath, K. V. S. Fire risk evaluation using multicriteria analysis-a case study. *Environ. Monit. Assess.* **166**(1–4), 223–239 (2010).
121. Pourghasemi, H. R., Beheshtirad, M. & Pradhan, B. A comparative assessment of prediction capabilities of modified analytical hierarchy process (M-AHP) and Mamdani fuzzy logic models using Netcad-GIS for forest fire susceptibility mapping. *Geom. Nat. Hazards Risk* **7**(2), 861–885 (2016).
122. Eskandari, S. A new approach for forest fire risk modeling using fuzzy AHP and GIS in Hyrcanian forests of Iran. *Arab. J. Geosci.* **10**(8), 190 (2017).
123. Vasconcelos, M. P., Silva, S., Tome, M., Alvim, M. & Pereira, J. C. Spatial prediction of fire ignition probabilities: comparing logistic regression and neural networks. *Photogramm. Eng. Remote Sens.* **67**, 73–81 (2001).
124. Massada, A. B., Syphard, A. D., Stewart, S. I. & Radeloff, V. C. Wildfire ignition-distribution modelling: a comparative study in the Huron-Manistee National Forest, Michigan, USA. *Int. J. Wildl. Fire* **22**, 174–183 (2013).
125. Leuenberger, M., Parente, J., Tonini, M., Pereira, M. G. & Kanevski, M. Wildfire susceptibility mapping: deterministic vs. stochastic approaches. *Environ. Modell. Softw.* **101**, 194–203 (2018).
126. Lozano, F. J., Suárez-Seoane, S., Kelly, M. & Luis, E. A multi-scale approach for modeling fire occurrence probability using satellite data and classification trees: a case study in a mountainous Mediterranean region. *Remote Sens. Environ.* **112**, 708–719 (2008).
127. Oliveira, S., Oehler, F., San-Miguel-Ayanz, J., Camia, A. & Pereira, J. M. C. Modeling spatial patterns of fire occurrence in Mediterranean Europe using multiple regression and 745 random forest. *For. Ecol. Manag.* **275**, 117–129 (2012).
128. Arpaci, A., Malowerschnig, B., Sass, O. & Vacik, H. Using multi variate data mining techniques for estimating fire susceptibility of Tyrolean forests. *Appl. Geogr.* **53**, 258–270 (2014).
129. Leuenberger, M., Kanevski, M., & Vega Orozco, C. D. Forest fires in a random forest. Geophysical Research Abstracts, Vol. 15, EGU General Assembly, 32–38 (2013).
130. Bui, T. D., Le, K. T., Nguyen, V., Le, H. & Revhaug, I. Tropical forest fire susceptibility mapping at the Cat Ba National Park area, Hai Phong City, Vietnam, using GIS-based Kernel logistic regression. *Remote Sens.* **8**(4), 347 (2016).
131. Breiman, L. Random forests. *Mach. Learn.* **45**, 5–32 (2001).
132. Bühler, Y. *et al.* Automated identification of potential snow avalanche release areas based on digital elevation models. *Nat. Hazards Earth Syst. Sci.* **13**, 1321–1335 (2013).
133. Bühler, Y. *et al.* Automated snow avalanche release area delineation–validation of existing algorithms and proposition of a new object-based approach for large-scale hazard indication mapping. *Nat. Hazards Earth Syst. Sci.* **18**, 1–10 (2018).
134. Bunn, A. G., Hughes, M. K. & Salzer, M. W. topographically modified tree-ring chronologies as a potential means to improve paleoclimate inference. *Clim. Chang.* **105**, 627–634 (2011).
135. Bui, D. T., Tuan, T. A., Klempe, H., Pradhan, B. & Revhaug, I. Spatial prediction models for shallow landslide hazards: a comparative assessment of the efficacy of support vector machines, artificial neural networks, kernel logistic regression, and logistic model tree. *Landslides* **13**, 361–378 (2016).
136. Bui, D. T. *et al.* A novel hybrid approach based on a swarm intelligence optimized extreme learning machine for flash flood susceptibility mapping. *CATENA* **179**, 184–196 (2019).
137. Cama, M., Lombardo, L., Conoscenti, C. & Rotigliano, E. Improving transferability strategies for debris flow susceptibility assessment: application to the Saponara and Itala catchments (Messina, Italy). *Geomorphology* **288**, 52–65 (2017).
138. Confortola, G., Maggioni, M., Freppaz, M. & Bocchiola, D. Modelling soil removal from snow avalanches: a case study in the North-Western Italian Alps. *Cold Reg. Sci. Technol.* **70**, 43–52 (2012).
139. Chen, W. *et al.* Spatial prediction of landslide susceptibility using data mining-based kernel logistic regression, naive Bayes and RBFNetwork models for the Long County area (China). *Bull. Eng. Geol. Environ.* **78**, 247–266 (2019).
140. Kim, K.-D., Lee, S. & Oh, H.-J. Prediction of ground subsidence in Samcheok City, Korea using artificial neural networks and GIS. *Environ. Geol.* **58**, 61–70 (2009).
141. Oh, H. J. & Lee, S. Integration of ground subsidence hazard maps of abandoned coal mines in Samcheok, Korea. *Int. J. Coal Geol.* **86**, 58–72 (2011).
142. Park, I., Lee, J. & Saro, L. Ensemble of ground subsidence hazard maps using fuzzy logic. *Open Geosci.* **6**, 207–218 (2014).
143. Massonnet, D. & Feigl, K. L. Radar interferometry and its application to changes in the Earth's surface. *Rev. Geophys.* **36**, 441–500 (1998).
144. Pilkington, S. & Mahmoud, H. Spatial and temporal variations in resilience to tropical cyclones along the United States coastline as determined by the multi-hazard hurricane impact level model. *Palgrave Commun.* **3**, 1–8 (2017).

145. Pilkington, S. F. & Mahmoud, H. N. Real-time application of the multihazard hurricane impact level model for the Atlantic Basin. *Front. Built Environ.* **3**, 67 (2017).
146. Pourghasemi, H. R., Gayen, A., Lasaponara, R. & Tiefenbacher, J. P. Application of learning vector quantization and different machine learning techniques to assessing forest fire influence factors and spatial modelling. *Environ. Res.* **1**, 109321 (2020).
147. Li, Z. G., Zhou, H. H. & Xu, Y. H. Research on prediction model of support vector machine based land subsidence caused by foundation pit dewatering. *Adv. Mater. Res.* **1**, 105–108 (2013).
148. Pham, B. T., Bui, D. T., Pourghasemi, H. R., Indra, P. & Dholakia, M. Landslide susceptibility assesssment in the Uttarakhand area (India) using GIS: a comparison study of prediction capability of naïve bayes, multilayer perceptron neural networks, and functional trees methods. *Theor. Appl. Climatol.* **128**, 255–273 (2017).
149. Huang, Y. & Zhao, L. Review on landslide susceptibility mapping using support vector machines. *CATENA* **165**, 520–529 (2018).
150. Arabameri, A., Pradhan, B., Rezaei, K. & Lee, C. W. Assessment of landslide susceptibility using statistical-and artificial intelligence-based FR–RF integrated model and multiresolution DEMs. *Remote Sens.* **11**, 999 (2019).
151. Yu, P.-S., Chen, S. T. & Chang, I. F. Support vector regression for real-time flood stage forecasting. *J. Hydrol.* **328**, 704–716 (2006).
152. Han, D., Chan, L. & Zhu, N. Flood forecasting using support vector machines. *J. Hydroinform.* **9**, 267–276 (2007).
153. Shi, Y., Taalab, K. & Cheng, T. Flood prediction using support vector machines (SVM) (2016).
154. Martínez, J., Chuvieco, E. & Martin, M. Estimating human risk factors in wildland fires in Spain using logistic regression: II. *International Symposium on Fire Economics, Planning and Policy: A Global Vision*. University of Cordoba, CD-Rom, Córdoba, 15 (2004).
155. Syphard, A. D. *et al.* Predicting spatial patterns of fire on a southern California landscape. *Int. J. Wildl. Fire* **17**, 602–613 (2008).
156. Martínez, J., Vega-Garcia, C. & Chuvieco, E. Human-caused wildfire risk rating for prevention planning in Spain. *J. Environ. Manage.* **90**, 1241–1252 (2009).
157. Mann, M. L. *et al.* Incorporating anthropogenic influences into fire probability models: effects of human activity and climate change on fire activity in California. *PLoS ONE* **11**, e0153589 (2016).
158. Zhang, Y., Lim, S. & Sharples, J. J. Modelling spatial patterns of wildfire occurrence in south-eastern Australia. *Geom. Nat. Hazards Risk* **7**, 1800–1815 (2016).
159. Syphard, A. D., Clarke, K. C. & Franklin, J. Simulating fire frequency and urban growth in southern California coastal shrublands, USA. *Landsc. Ecol.* **22**, 431–445 (2007).
160. Chuvieco, E. *et al.* Development of a framework for fire risk assessment using remote sensing and geographic information system technologies. *Ecol. Model.* **221**, 46–58 (2010).
161. Bell, R. & Glade, T. Multi-hazard analysis in natural risk assessments. *Landslides* **1**, 1–10 (2012).

Acknowledgments

This work was supported by College of Agriculture, Shiraz University (Grant No. 98GRC1M271143). Authors would like to thank from Dr. OLivier Jaquet, another anonymous reviewer, and Editorial Board Member (Susanna Falsaperla) comments.

Author contributions

S.Y., H.R.P., S.N.E., S.P., S.E., and J.P.T. designed experiments, run models, analyzed results, wrote and reviewed manuscript. All authors reviewed the final manuscript.

Competing interests

The authors declare no competing interests.

Additional information

Correspondence and requests for materials should be addressed to H.R.P.

Reprints and permissions information is available at www.nature.com/reprints.

Publisher's note Springer Nature remains neutral with regard to jurisdictional claims in published maps and institutional affiliations.